

2023-09-07

Tropical forests are approaching critical temperature thresholds

Doughty, CE

<https://pearl.plymouth.ac.uk/handle/10026.1/21658>

10.1038/s41586-023-06391-z

Nature

Springer Science and Business Media LLC

All content in PEARL is protected by copyright law. Author manuscripts are made available in accordance with publisher policies. Please cite only the published version using the details provided on the item record or document. In the absence of an open licence (e.g. Creative Commons), permissions for further reuse of content should be sought from the publisher or author.

Tropical forests are approaching critical temperature thresholds

Christopher E. Doughty¹, Jenna Keany¹, Benjamin C. Wiebe¹, Camilo Rey-Sanchez², Kelsey R. Carter^{3,3.5}, Kali B. Middleby⁴, Alexander W. Cheesman⁴, Michael L. Goulden⁵, Humberto R. da Rocha⁶, Scott D. Miller⁷, Yadvinder Malhi⁸, Sophie Fauset⁹, Emanuel Gloor¹⁰, Martijn Slot¹¹, Imma M. Oliveras Menor^{8,12}, Kristine Y. Crous¹³, Gregory R. Goldsmith¹⁴, Joshua B. Fisher¹⁴

¹School of Informatics, Computing, and Cyber Systems, Northern Arizona University, Flagstaff, AZ, USA

² Department of Marine, Earth and Atmospheric Sciences, North Carolina State University, Raleigh, NC, USA

³ College of Forest Resources and Environmental Sciences, Michigan Technological University, Houghton, MI, USA

^{3.5} Earth and Environmental Sciences Division, Los Alamos National Laboratory, Los Alamos, NM, USA

⁴ Centre for Tropical Environmental and Sustainability Science, James Cook University, Cairns, QLD, Australia

⁵Department of Earth System Science, University of California, Irvine, California, USA

⁶Departamento de Ciências Atmosféricas, Universidade de São Paulo, São Paulo, Brazil

⁷Atmospheric Sciences Research Center, State University of New York at Albany, Albany, NY, USA

⁸Environmental Change Institute, School of Geography and the Environment, University of Oxford, Oxford, UK

⁹School of Geography, Earth and Environmental Sciences, University of Plymouth, Plymouth, UK

¹⁰University of Leeds, Leeds, UK

¹¹ Smithsonian Tropical Research Institute, Balboa Ancon, Republic of Panama

¹² AMAP (Botanique et Modélisation de l'Architecture des Plantes et des Végétations), CIRAD, CNRS, INRA, IRD, Université de Montpellier, Montpellier, France

¹³Western Sydney University, Hawkesbury Institute for the Environment, Penrith, NSW, Australia

¹⁴Schmid College of Science and Technology, Chapman University, Orange, CA 92866 USA

Keywords –climate change, ECOSTRESS, photosynthesis, Tcrit, temperature, tree mortality, warming

34

35 **Abstract** –The critical temperature beyond which photosynthetic machinery in tropical trees
36 begins to fail averages $\sim 46.7^{\circ}\text{C}$ (T_{crit})¹. However, it remains unclear whether leaf temperatures
37 experienced by tropical vegetation approach this threshold or soon will under climate change.
38 We found that pantropical canopy temperatures independently triangulated from individual leaf
39 thermocouples, pyrgeometers, and remote sensing (ECOSTRESS) have midday-peak
40 temperatures of $\sim 34^{\circ}\text{C}$ during dry periods, with a long high-temperature tail that can exceed
41 40°C . Leaf thermocouple data from multiple sites across the tropics suggest that even within
42 pixels of moderate temperatures, upper-canopy leaves exceed T_{crit} 0.01% of the time. Further,
43 upper-canopy leaf warming experiments (+2, 3, and 4°C in Brazil, Puerto Rico and Australia)
44 increased leaf temperatures non-linearly with peak leaf temperatures exceeding T_{crit} 1.3% of the
45 time (11% $>43.5^{\circ}\text{C}$, 0.3% $>49.9^{\circ}\text{C}$). Using an empirical model incorporating these dynamics
46 (validated with warming experiment data), we found that tropical forests can withstand up to a
47 $3.9 \pm 0.5^{\circ}\text{C}$ increase in air temperatures before a potential tipping point in metabolic function,
48 but remaining uncertainty in the plasticity and range of T_{crit} in tropical trees and the impact of
49 leaf death on tree death could drastically change this prediction. The 4.0°C estimate is within the
50 “worst case scenario” (RCP-8.5) of climate change predictions² for tropical forests and therefore
51 it is still within our power to decide (e.g., by not taking the RCP 6.0 or 8.5 route) the fate of these
52 critical realms of carbon, water, and biodiversity^{3,4}.

53

54

55

56

57 **Introduction**

58 Tropical forest mean temperatures are high, and their diel and seasonal variations are relative
59 small, thus even a small change in temperature could more greatly impact tropical plant species
60 than a large temperature change in other global regions⁵. Average temperatures have risen by
61 0.5 °C per decade in some tropical regions, and temperature extremes are becoming more
62 pronounced (e.g. the El Niño of 2015 was 1.5 °C warmer than the El Niño of 1997)^{6,7}. Since
63 temperatures in tropical forests are near or above the temperature optimum for photosynthesis⁸,
64 further increased temperatures may close stomata, reducing transpirational cooling and exposing
65 leaves to damaging temperatures. More than 150 years ago, Sachs (1864) first reported that
66 leaves from different plant species could withstand temperatures up to 50 °C, but would die at
67 temperatures even slightly higher⁹. In the era of climate change, this finding is still relevant.
68 How close are forests to a high temperature threshold such as the one proposed by Sachs?
69 Nowhere is such a question more pressing than in tropical forests, which serve as critical stores
70 and sinks of carbon, play host to most of the world's biodiversity, and may be more sensitive to
71 increasing temperatures than other ecoregions^{3,4}.

72 More recently, techniques to determine the ability for leaves to withstand high temperatures have
73 advanced to focus on T_{crit} , or the temperature at which irreversible damage to the photosynthetic
74 machinery occurs. Over the past few years, T_{crit} data have become increasingly available for
75 tropical forests, specifically measured as the temperature at which the ratio of variable
76 fluorescence yield to maximum fluorescence yield (F_v/F_m), reflecting photosystem II
77 functioning, starts to decline^{1,10}. The decline in F_v/F_m is often followed by development of
78 necrosis and leaf death¹¹. Heat tolerance, measured by T_{crit} , varies minimally among tropical
79 species, mainly due to differences in growing environment and leaf traits. For instance, among
80 147 tropical tree species, the average T_{crit} was found to be 46.7 °C (5th–95th percentile: 43.5–49.7
81 °C)¹. They also found that older tree lineages that experienced higher temperatures in the
82 distant past did not have higher T_{crit} and thus, were not better acclimated to higher temperatures
83 today. Across the planet, heat tolerance generally increases with higher mean growing
84 temperatures. For example, as average temperatures increase by ~20 °C from the Arctic to the
85 Tropics, heat tolerance was 9 °C greater in tropical plants than arctic plants¹². Similarly, as
86 temperatures decrease by 17 °C along a tropical elevation gradient, heat tolerance decreases by
87 ~2 °C¹⁰. Heat tolerance also increases with increasing leaf mass area (LMA), suggesting that
88 heat tolerance may be linked to construction costs of the leaves and their mean leaf lifetime¹.

89 With a much-improved understanding of T_{crit} across the Tropics, it is now important to know
90 how close tropical leaves are to experiencing and surpassing these critical temperatures. In the
91 past, tropical forest leaf and canopy temperatures were difficult and time consuming to measure,
92 but new technologies like drones and thermal cameras are making the process much easier¹³.
93 More recently, the ECOsystem Spaceborne Thermal Radiometer Experiment on Space Station
94 (ECOSTRESS) sensor on the International Space Station (ISS) can provide unique high temporal
95 and spatial resolution measurements of land surface temperatures at the global scale¹⁴.
96 ECOSTRESS is an improvement over previous thermal satellite land surface temperature (LST)
97 sensors because it has 5 spectral bands, a 70 m spatial resolution, and multiple diel overpass
98 times, as well as improved algorithms.

99 Here we use data from the new ECOSTRESS sensor to estimate peak pantropical forest canopy
100 temperatures. We begin by ground truthing the satellite data with tower-based pyrgeometer data.
101 We then use these data to determine what causes variation in peak temperatures at the canopy
102 scale and show similar trends driving peak temperatures across all of the Tropics. Critically, we
103 show that for a given canopy temperature, individual leaf temperatures display a “long tail” of
104 values in the distribution, where the temperatures of a few individual leaves far exceed that of
105 the overall canopy, and that this skewed distribution persists under leaf warming experiments of
106 2, 3 and 4 °C. Finally, we develop a simple empirical model to explore the implications of
107 observed leaf temperatures on the fate of tropical forests under future climate change.

108

110 *Ground validation* using pyrgeometer data- We first ground-truth ECOSTRESS and find similar
111 peak temperatures between a 3-year, 30-minute averaged canopy temperature pyrgeometer
112 dataset for a lowland tropical rainforest site near the Tapajos River (KM 83) in Brazil and a
113 broad region (Fig ED1a red box) of the Amazon Basin (Fig 1a; $r^2 = 0.75$, $N=16$, $P < 0.0001$, with
114 ECOSTRESS having a slight cool bias (Fig ED2d) matching previous findings¹⁵). The
115 pyrgeometer data at that site indicate that midday sunny canopy temperatures in the dry season
116 (July to Dec) averaged 33.5 °C compared to 31.0 °C in the wet season (Jan to June) (Fig 1a).
117 Sampling frequency (Fig ED3), latent heat flux (Fig ED 2c), air temperature (Fig ED2b), and soil
118 moisture (Fig ED2a) all impacted canopy temperatures. The tower-mounted pyrgeometer
119 inherently averages spatially (over an 8,000 m² footprint) and thus amalgamates individual peak
120 leaf temperatures. Therefore, we used leaf thermocouples on three canopy tree species at the
121 same site to assess individual leaf temperatures. The mean temperatures for 11 individual sun-
122 exposed leaves over 54 sunny 20-minute periods also averaged ~33.2 °C (similar to that
123 measured by the pyrgeometer) but with a “long tail” of high temperatures (> 40 °C) in the
124 distribution (Fig 1b).

125 We then aggregated similar upper-canopy leaf thermocouple datasets from Brazil¹⁶¹⁷, Puerto
126 Rico¹⁸, Panama¹⁹ and Australia²⁰ and all had “long tail distributions” (Fig 1c and ED4-5) with
127 upper limits ~44 °C (43-48) (but see Fig ED5c for a cooler Atlantic forest example¹⁶). When we
128 zoom in on the long tail of each dataset (insets in Fig ED4-5), the curve shows statistical
129 regularity, which allows us to estimate T_{crit} as a percent of all canopy top leaves. For instance,
130 when all data are aggregated across sites, we estimate that 0.01% (0.03% >43.5°C) of all leaves
131 will surpass T_{crit} at least once a season (Fig 1c). Although infrequent, the occurrence of extreme
132 temperatures may have a catastrophic effect on a leaf’s physiology and may be thought of as a
133 low probability, high impact event.

134 We then aggregated data from three in situ upper-canopy warming experiments where leaves
135 were heated by 2, 3, and 4 °C (in Brazil¹⁷, Puerto Rico¹⁸, and Australia²⁰ respectively). Warmed
136 leaf peak temperatures ranged between 51-54 °C (Fig ED4), an increase of ~8 °C above ambient
137 highs (mean ~45 °C-; Fig ED4). The percentage of warmed leaves exceeding T_{crit} at least once a
138 year increased to 1.3% of all warmed leaves (11% >43.5°C, 0.3% >49.9°C) (Fig 1c), because of
139 a non-linear relationship between leaf and air temperatures in the warming experiments (Fig 1d).
140 During the Brazilian warming experiment, individual leaves exceeded T_{crit} and T_{50} with
141 noticeable signs of leaf necrosis, some for a duration of >8 mins (Fig ED6), and following this,
142 net transpiration in warmed branches decreased significantly ($P < 0.0001$) by an average of 27%
143 (Fig 3a). In the warming experiments, leaves exceeded T_{crit} for extended periods (>8 minutes)
144 0.2% (0.6% for >6 minutes) of the time over the course of a season (Fig ED6), events that can
145 cause leaf browning and necrosis.

146 *Remote sensing data* – We analyze ECOSTRESS LST data along with comparisons to VIIRS
147 and MODIS, as well as SMAP soil moisture. At the landscape scale (Fig ED1 red box), peak
148 ECOSTRESS LST (~36 °C) using all data corresponded with periods of low SMAP-measured
149 soil moisture (~0.3 m³ m⁻³) (Fig 2a and b). A linear extrapolation of our pyrgeometer data to a
150 soil moisture of 0.3 m³ m⁻³ would predict a similar canopy temperature (~36 °C) (Fig ED2a). For
151 the warmest datapoint (Fig 2c and d), we then expanded the area (Fig ED1 blue box) and applied
152 the highest quality data flags (~6% of the data used – see methods and SI for an extensive

153 discussion of this), which reduced the median value to 34 °C. These average temperatures do not
154 reflect the extremes, as 0.5% of the data is >38 °C and 0.1% is > 40 °C (Fig 2d and Table 1).
155 We show the long tail distribution of temperatures (with a log10 scale) for Amazonia in Fig 2d.
156 Using less restrictive or no quality flags generally resulted in higher tails > 40 °C (Table S2). We
157 compare ECOSTRESS to other LST satellites (VIIRS, MODIS) (Fig ED9-10 and Table S1-2)
158 and show similar results, but with greater fidelity and ability to capture long tails with
159 ECOSTRESS. LST for Central Africa (Fig 2e and Fig ED7) and SE Asia (Fig 2f and Fig ED8)
160 during similar peak dry periods had similar peak temperatures (with data flags; Table 1). We
161 then estimated the highest temperatures during dry periods if temperature increased by 2 °C (to
162 simulate climate change) and found that the percent of time above threshold temperatures would
163 increase by an order of magnitude in all three regions. For example, the percent time Amazon
164 canopies spend at temperatures ≥ 38.0 °C would increase from 0.5 to 5% and the percent time \geq
165 40.0 °C would increase from 0.1 to 1% (Table 1).

166 *Model results* - An empirical model to explore the temperature thresholds of tropical trees was
167 parameterized using the temperature distributions of warmed and non-warmed leaves (Fig 1c)
168 from the combined tropical datasets (N=5). Assuming leaf death at T_{crit} , and evaporative cooling
169 as a linear function of the number of leaves, we show that enhanced warming could tip the forest
170 towards the death of all leaves and possible tree mortality (Fig 3b and Table 2). The modelled
171 impact of warming on reduced transpirational cooling approximately matched the measured
172 values; a 26 (± 28) % (N=30 simulations) reduction of modelled evaporative cooling with ~ 2 °C
173 warming, versus a measured 27% average reduction after ~ 2 °C warming during the Brazilian
174 warming experiment (Fig 3a). The decline in transpiration occurred after leaf temperatures
175 exceeding both T_{crit} for >8 mins (Fig 3a inset) and T_{50} . Mean initial modelled canopy
176 temperature was 33.7 ± 0.4 °C, matching the measured canopy average (33.5 °C) during peak
177 temperature periods (sunny, midday). When run using the most likely parameters, including a
178 T_{crit} of 46.7 °C¹, the model showed that most forests could withstand up to 3.9 ± 0.5 °C warming
179 before the death of all leaves and potential tree death (n =30 simulation runs; Fig 3b and Table
180 2), but a series of sensitivity studies give a temperature distribution between 2-8 °C (Table 2).
181 Due to the stochastic nature of droughts in our model, total leaf loss ranged over a wide
182 timespan. For instance, if temperatures increase by 0.03 °C per year, we estimate that the mean
183 time to leaf death would be 132 years, but extensive canopy leaf mortality could occur as early as
184 102 years and as late as 163 years (Fig 3b and Table 2).

185

186

187 Discussion

188 Several lines of remotely sensed, tower-based, and *in situ* evidence (ECOSTRESS,
189 VIIRS, pyrgeometer, leaf thermocouples) suggest that hot periods in tropical forests with low
190 soil moisture lead to canopy temperatures that average ~ 34 °C, with some pixels exceeding 40
191 °C^{8,21}. Even within a given LST pixel, there is a long tail distribution with individual leaf
192 temperatures exceeding 40 °C. Currently, 0.01% of upper canopy leaves from *in situ*
193 measurements exceed T_{crit} at least once a season (N=5 sites); warming experiments (N=3)
194 suggest 1.4% will exceed T_{crit} under future warming conditions (Figs S7-9). We posit that
195 capturing the higher tail temperatures may be important for future climate change predictions in
196 tropical forests because as individual leaves exceed T_{crit} , they die, thus reducing the net
197 evaporative cooling potential for the canopy, as suggested in Fig 1d and 3a). This is supported
198 by branch warming experiments where noticeable signs of leaf damage and a reduction of
199 transpiration by 27% followed periods where leaf temperatures exceeded T_{crit} for extended
200 periods (Fig 3a). Certain tropical regions, such as the Southeast Amazon, may already be
201 experiencing critical thresholds²². Many recent large-scale drought studies have shown that the
202 largest, most sun-exposed trees die disproportionately^{23,24}. Moreover, there has been a recent
203 increase in continental mortality rates across the Amazon basin (although not in the Congo basin
204 and Table 1 shows the Congo basin experiences lower peak temperatures than the Amazon)⁴ and
205 carbon uptake across the basin has been reduced²⁵. We propose that high leaf temperatures may
206 play a role (along with carbon starvation and hydraulic limitation³⁴) in those recent mortality
207 events.

208 We make several assumptions in our model related to the broader tipping point results.
209 The first key assumption is that within a given LST pixel, there is a long tail of high individual
210 tropical leaf temperatures following Fig 1c. This is supported by several leaf thermocouple
211 datasets (N=5, Fig 1, (Figs S7-9)), all of which show a long-tail, as well as first principles (SI
212 text). Critically, warming experiments show non-linear trends (Fig 1c and d) where temperature
213 increases of 2, 3, and 4 °C increase maximum leaf temperatures by larger amounts (+8.1 °C, +6.1
214 °C, 8.0 °C, respectively; Fig ED4). Many other studies have documented individual leaf
215 temperatures approaching 46.7 °C^{8,11,16,19}.

216 The second assumption is that water-stressed pantropical median canopy temperatures
217 can average ~ 34 °C with a spatial tail exceeding 40 °C (Fig 2). In other words, RS data suggest
218 entire canopies and forests getting very warm and (our first assumption) that within these pixels,
219 there is a long-tail distribution of individual leaf temperatures. ECOSTRESS and VIIRS LST
220 data are both >1 °C warmer (34.7 and 33.9 °C) than older LST sensors like MODIS (32.7 °C)
221 (ECOSTRESS has ~ 0.75 °C cold bias compared to VIIRS¹⁵). We assume ECOSTRESS and
222 VIIRS will be more accurate than MODIS because there are more thermal bands, vegetation can
223 be identified with emissivity (for ECOSTRESS and VIIRS, but not MODIS), and an improved
224 algorithm²⁶ can accurately estimate temperatures within 1 K for many surfaces²⁷. We further
225 found that adding 2 °C (to replicate climate change) to the measured ECOSTRESS satellite data
226 would increase the occurrence of high tail temperatures by about an order of magnitude (e.g.,
227 from 0.1 to 1% > 40 °C) (Table 1). Therefore, the change in percentage of time when
228 temperatures exceeded >40 °C in response to a simple addition of 2 °C was not a simple linear
229 change.

230 The third assumption is that leaves at temperatures $> T_{crit}$ will die, and thus stop
231 contributing to future transpiration (although transpiration often stops at temperatures lower than

232 T_{crit}), and that the sum of evaporative cooling is a linear function of the total number of
233 transpiring leaves. Our T_{crit} value is based on Slot et al. (2021), who found the mean (T_{crit}) was
234 46.7 °C (5th–95th percentile: 43.5–49.7 °C) and the temperature when F_v/F_m had decreased by
235 50% (T_{50}) was 49.9 °C (47.8–52.5 °C)¹. T_{crit} variation is important because ~50% of the species
236 from Slot et al. (2021) had a T_{crit} <46.7 °C with negative consequences at lower temperatures for
237 those species. Incorporating this variation in our model demonstrated those consequences can
238 exacerbate conditions for other species as they die and their evaporative cooling is reduced,
239 leading to less future warming (~0.1 °C) needed to achieve leaf death when such variation is
240 included (Table 2). Branch warming experiments in Brazil showed large (27%) decreases in
241 transpiration when leaves reached either T_{50} or T_{crit} for an extended period (>8 minutes) (Fig 3).
242 It was not possible to determine which (T_{50} , extended T_{crit} , or a different variable) was more
243 critical for the decrease in transpiration in our dataset (but another recent study found leaf death
244 when leaf temperatures exceeded T_{crit} for between 10 and 40 minutes²⁸). If a longer time is
245 necessary to exceed T_{crit} prior to leaf death, T_{crit} will be exceeded less often and our model
246 suggests that the forest canopies could resist an additional 0.7 °C increase in air temperatures
247 prior to leaf death (Table 2). Prior work had suggested that irreversible damage will often occur
248 at 45–60 °C²⁹.

249 T_{crit} was the largest source of uncertainty in the model and changed the tipping point
250 temperatures by between 2–8 °C (Table 2). T_{crit} has been adopted because it is relatively easy to
251 measure and can be standardized across ecosystems. However, the impact of T_{crit} on plant
252 hydraulics still needs more research³⁰. Other uncertainties include the importance of T_{crit} vs T_{50}
253 on enzyme denaturation and how long exposure to high temperatures is needed for enzyme
254 denaturation to occur¹. We also assumed that T_{crit} does not acclimate to warming—acclimation
255 has been observed in temperate species³¹, but the few studies that examined acclimation in
256 tropical species, found no, or very limited evidence for upregulation of T_{crit} ^{11, 32} (although warm
257 selected tropical trees in Biosphere 2 did show acclimation of T_{crit} ³³). In a sensitivity study we
258 allowed acclimation by enabling leaves to increase T_{crit} by 0.5 °C or 1 °C, which increased forest
259 resistance to warming by similar amounts (by 0.5 °C and 1 °C).

260 An additional assumption was that if all leaves die at T_{crit} , the tree will die. However,
261 tropical trees may use non-structural carbohydrate (NSC)^{34,35} reserves to reflush leaves in later
262 years, but this is highly uncertain. Given these uncertainties, we made the simple assumption that
263 leaf level T_{crit} is a general signal of enzyme denaturation (supported by³⁶), which will have a
264 range of other impacts including reducing evaporative cooling and possibly leading to tree death.
265 It is clear that further studies are needed. However, in a sensitivity study, we tried to account for
266 high NSCs by allowing trees to reflush an LAI of 2 (e.g. increase total LAI to 7) which slightly
267 increased resilience by 0.2 °C (SI text). We also assume that all sunlit leaves have an equal
268 chance of dying, but leaf orientation likely impacts both leaf temperatures and T_{crit} and only
269 further studies may address this. If the assumptions above are robust, then our model suggests
270 that tropical forests may be approaching a high temperature threshold.

271 How close are future predictions of temperature increases in tropical forests to our
272 predictions of leaf death? An ensemble of CMIP5 models (with similar results from CMIP6³⁷),
273 the “worst case scenario” (RCP 8.5), predicts temperature increases of 3.3 ± 0.6 °C by 2081–
274 2100 for tropical regions with land regions heating by ~5 °C by 2181 in RCP 6.0 and by 2081 in
275 RCP 8.5². This level of climate change is within the range of our most likely scenario of $3.9 \pm$
276 0.50 °C of temperature increases that lead to a tipping point. However, the 4 °C is out of the

277 range of the “best case scenario” (RCP 2.6) of 0.9 ± 0.3 °C, or 1.4 ± 0.5 °C for the land surface.
278 Tree death could come earlier through a combination of mechanisms and their interactions (e.g.,
279 carbon starvation, hydraulic limitation, fire, etc.). Further, even at lower temperatures, partial
280 canopy death can negatively affect CO₂ uptake feedbacks, which could accelerate climate change
281 effects. Our sensitivity study (Table 2) shows temperature ranges leading to leaf death between
282 ~ 2.0 and 8.1 °C (the lowest and highest scenarios plus error). Scenario uncertainty due to the
283 change in drought prevalence played a relatively small role, shifting our best estimate by ~0.4
284 °C. Most of this uncertainty is methodological (T_{crit} value and high temperature duration), which
285 could be reduced with further studies and method standardization of T_{crit} measurements.

286 **Conclusion** –Our work suggests that a tipping point in metabolic function in tropical forests
287 could occur with 3.9 ± 0.5 °C of additional warming, which is more than expected for tropical
288 forests under RCP 2.6, but less than under RCP 6.0 or 8.5. We use T_{crit} to simplify an
289 enormously complex process and we want to emphasize that even our great uncertainty (2-8 °C)
290 estimates may ignore critical feedbacks such as sensitivity of reproduction to high temperatures,
291 hydraulic failure due to embolisms, and more generally, other unexplored positive feedback
292 loops. Recent literature suggests a resilience of tropical forests to how warming impacts carbon
293 uptake³³ (but see²⁵) and long-term drought³⁸. However, T_{crit} acts as an absolute upper limit and
294 it seems that, if our assumptions in the model are correct, crossing such a threshold is within the
295 range of our most pessimistic future climate change scenarios (RCP 6.0 or 8.5). In addition,
296 deforestation and fragmentation can amplify local temperature changes³⁹. The combination of
297 climate change and local deforestation may already be placing the hottest tropical forest regions
298 close to, or even beyond, a critical thermal thresholds⁴⁰. Therefore, our results suggest the
299 combination of ambitious climate change mitigation goals and reduced deforestation can ensure
300 that these important realms of carbon, water, and biodiversity^{3,4} stay below thermally critical
301 thresholds.

302

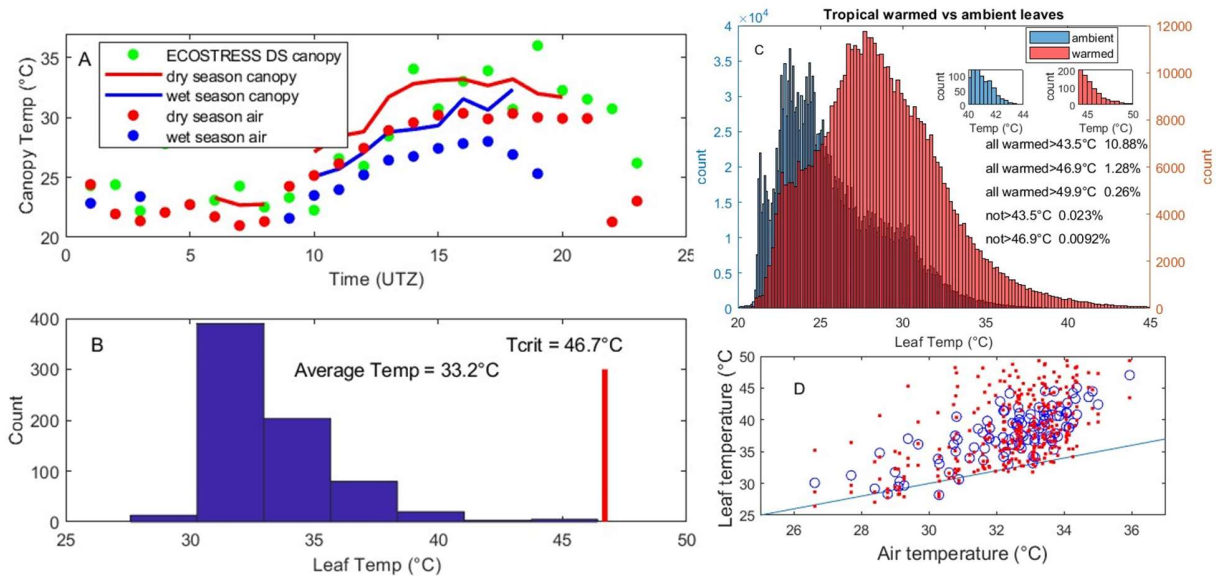
304 **References**

- 305 1. Slot, M. *et al.* Leaf heat tolerance of 147 tropical forest species varies with elevation and
 306 leaf functional traits, but not with phylogeny. *Plant. Cell Environ.* **44**, (2021).
- 307 2. Collins, M., R., Knutti, J., Arblaster, J.-L., Dufresne, T. & Fichet. Long-term Climate
 308 Change: Projections, Commitments and Irreversibility. in *Climate Change 2013: The*
 309 *Physical Science Basis. Contribution of Working Group I to the Fifth Assessment Report*
 310 *of the Intergovernmental Panel on Climate Change* (Cambridge University Press).
- 311 3. Wilson, E. & Raven, P. *Our diminishing tropical forests. Biodiversity.* ((National
 312 Academy Press, 1988).
- 313 4. Hubau, W. *et al.* Asynchronous carbon sink saturation in African and Amazonian tropical
 314 forests. *Nature* (2020) doi:10.1038/s41586-020-2035-0.
- 315 5. Janzen, D. H. Why Mountain Passes are Higher in the Tropics. *Am. Nat.* **101**, 233–249
 316 (1967).
- 317 6. Jiménez-Muñoz, J. C. *et al.* Record-breaking warming and extreme drought in the
 318 Amazon rainforest during the course of El Niño 2015–2016. *Sci. Rep.* **6**, 33130 (2016).
- 319 7. Jiménez-Muñoz, J. C., Sobrino, J. A., Mattar, C. & Malhi, Y. Spatial and temporal
 320 patterns of the recent warming of the Amazon forest. *J. Geophys. Res. Atmos.* **118**, 5204–
 321 5215 (2013).
- 322 8. Doughty, C. E. & Goulden, M. L. Are tropical forests near a high temperature threshold?
 323 *J. Geophys. Res. Biogeosciences* (2009) doi:10.1029/2007JG000632.
- 324 9. Sachs, J. Über die obere Temperaturgränze der Vegetation. *Flora* **47**, 5–12 (1864).
- 325 10. Feeley, K. *et al.* The Thermal Tolerances, Distributions, and Performances of Tropical
 326 Montane Tree Species . *Frontiers in Forests and Global Change* vol. 3 25 (2020).
- 327 11. Krause, G. H. *et al.* High-temperature tolerance of a tropical tree, *Ficus insipida*:
 328 methodological reassessment and climate change considerations. *Funct. Plant Biol.* **37**,
 329 890–900 (2010).
- 330 12. O’sullivan, O. S. *et al.* Thermal limits of leaf metabolism across biomes. *Glob. Chang.*
 331 *Biol.* **23**, 209–223 (2017).
- 332 13. Still, C. J. *et al.* Imaging canopy temperature: shedding (thermal) light on ecosystem
 333 processes. *New Phytol.* **n/a**, (2021).
- 334 14. Fisher, J. B. *et al.* ECOSTRESS: NASA’s Next Generation Mission to Measure
 335 Evapotranspiration From the International Space Station. *Water Resour. Res.* **56**,
 336 e2019WR026058 (2020).
- 337 15. Hulley, G. C. *et al.* Validation and Quality Assessment of the ECOSTRESS Level-2 Land
 338 Surface Temperature and Emissivity Product. *IEEE Trans. Geosci. Remote Sens.* **60**, 1–23
 339 (2022).
- 340 16. Fauset, S. *et al.* Differences in leaf thermoregulation and water use strategies between
 341 three co-occurring Atlantic forest tree species. *Plant. Cell Environ.* **41**, 1618–1631 (2018).
- 342 17. Doughty, C. E. An In Situ Leaf and Branch Warming Experiment in the Amazon.
 343 *Biotropica* **43**, 658–665 (2011).
- 344 18. Carter, K. R., Wood, T. E., Reed, S. C., Butts, K. M. & Cavaleri, M. A. Experimental
 345 warming across a tropical forest canopy height gradient reveals minimal photosynthetic
 346 and respiratory acclimation. *Plant. Cell Environ.* **44**, 2879–2897 (2021).
- 347 19. Rey-Sanchez, A. C., Slot, M., Posada, J. & Kitajima, K. Spatial and seasonal variation of
 348 leaf temperature within the canopy of a tropical forest. *Clim. Res.* **71**, 75–89 (2016).

- 349 20. Crous, K. Y. *et al.* Similar patterns of leaf temperatures and thermal acclimation to
350 warming in temperate and tropical tree canopies. *Tree Physiol.* tpad054 (2023)
351 doi:10.1093/treephys/tpad054.
- 352 21. Kivalov, S. N. & Fitzjarrald, D. R. Observing the Whole-Canopy Short-Term Dynamic
353 Response to Natural Step Changes in Incident Light: Characteristics of Tropical and
354 Temperate Forests. *Boundary-Layer Meteorol.* **173**, 1–52 (2019).
- 355 22. Tiwari, R. *et al.* Photosynthetic quantum efficiency in south-eastern Amazonian trees may
356 be already affected by climate change. *Plant. Cell Environ.* **n/a**, (2020).
- 357 23. da Costa, A. C. L. *et al.* Effect of 7 yr of experimental drought on vegetation dynamics
358 and biomass storage of an eastern Amazonian rainforest. *New Phytol.* (2010)
359 doi:10.1111/j.1469-8137.2010.03309.x.
- 360 24. Phillips, O. L. *et al.* Drought sensitivity of the amazon rainforest. *Science (80-.).* (2009)
361 doi:10.1126/science.1164033.
- 362 25. Gatti, L. V *et al.* Amazonia as a carbon source linked to deforestation and climate change.
363 *Nature* **595**, 388–393 (2021).
- 364 26. Hulley, G. C. & Hook, S. J. Generating Consistent Land Surface Temperature and
365 Emissivity Products Between ASTER and MODIS Data for Earth Science Research. *IEEE*
366 *Trans. Geosci. Remote Sens.* **49**, 1304–1315 (2011).
- 367 27. Gillespie, A. *et al.* A temperature and emissivity separation algorithm for Advanced
368 Spaceborne Thermal Emission and Reflection Radiometer (ASTER) images. *IEEE Trans.*
369 *Geosci. Remote Sens.* **36**, 1113–1126 (1998).
- 370 28. Kitudom, N. *et al.* Thermal safety margins of plant leaves across biomes under a
371 heatwave. *Sci. Total Environ.* **806**, 150416 (2022).
- 372 29. Berry, J. & Bjorkman, O. Photosynthetic Response and Adaptation to Temperature in
373 Higher Plants. *Annu. Rev. Plant Physiol.* **31**, 491–543 (1980).
- 374 30. Blonder, B. & Michaletz, S. T. A model for leaf temperature decoupling from air
375 temperature. *Agric. For. Meteorol.* **262**, 354–360 (2018).
- 376 31. Drake, J. E. *et al.* Trees tolerate an extreme heatwave via sustained transpirational cooling
377 and increased leaf thermal tolerance. *Glob. Chang. Biol.* **24**, 2390–2402 (2018).
- 378 32. Guha, A. *et al.* Short-term warming does not affect intrinsic thermotolerance but induces
379 strong sustaining photoprotection in tropical evergreen citrus genotypes. *Plant. Cell*
380 *Environ.* **45**, 105–120 (2022).
- 381 33. Smith, M. N. *et al.* Empirical evidence for resilience of tropical forest photosynthesis in a
382 warmer world. *Nat. Plants* **6**, 1225–1230 (2020).
- 383 34. Doughty, C. E. *et al.* Drought impact on forest carbon dynamics and fluxes in Amazonia.
384 *Nature* (2015) doi:10.1038/nature14213.
- 385 35. Dickman, L. T. *et al.* Homeostatic maintenance of nonstructural carbohydrates during the
386 2015–2016 El Niño drought across a tropical forest precipitation gradient. *Plant. Cell*
387 *Environ.* **42**, 1705–1714 (2019).
- 388 36. Subasinghe Achchige, Y. M., Volkova, L., Drinnan, A. & Weston, C. J. A quantitative test
389 for heat-induced cell necrosis in vascular cambium and secondary phloem of *Eucalyptus*
390 *obliqua* stems. *J. Plant Ecol.* **14**, 160–169 (2021).
- 391 37. Tebaldi, C. *et al.* Climate model projections from the Scenario Model Intercomparison
392 Project (ScenarioMIP) of CMIP6. *Earth Syst. Dyn.* **12**, 253–293 (2021).
- 393 38. Rowland, L. *et al.* Death from drought in tropical forests is triggered by hydraulics not
394 carbon starvation. *Nature* (2015) doi:10.1038/nature15539.

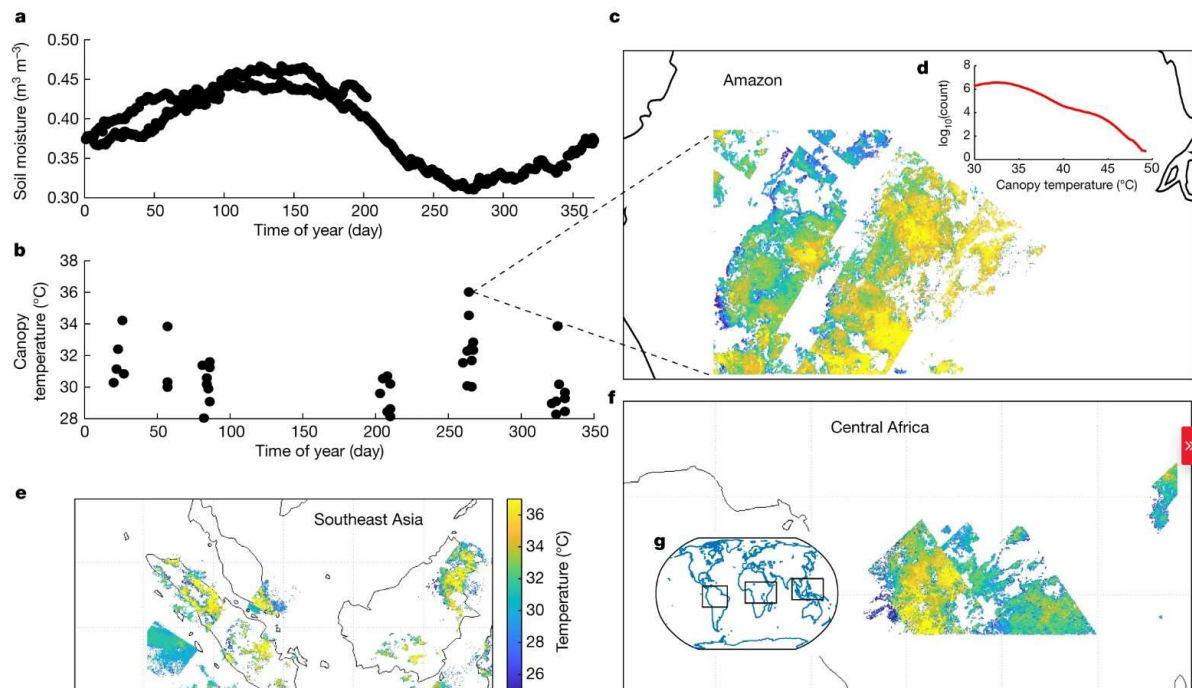
- 395 39. Vargas Zeppetello, L. R. *et al.* Large scale tropical deforestation drives extreme warming.
396 *Environ. Res. Lett.* **15**, 84012 (2020).
- 397 40. Araújo, I. *et al.* Trees at the Amazonia-Cerrado transition are approaching high
398 temperature thresholds. *Environ. Res. Lett.* **16**, 34047 (2021).
399

400 **Figures**



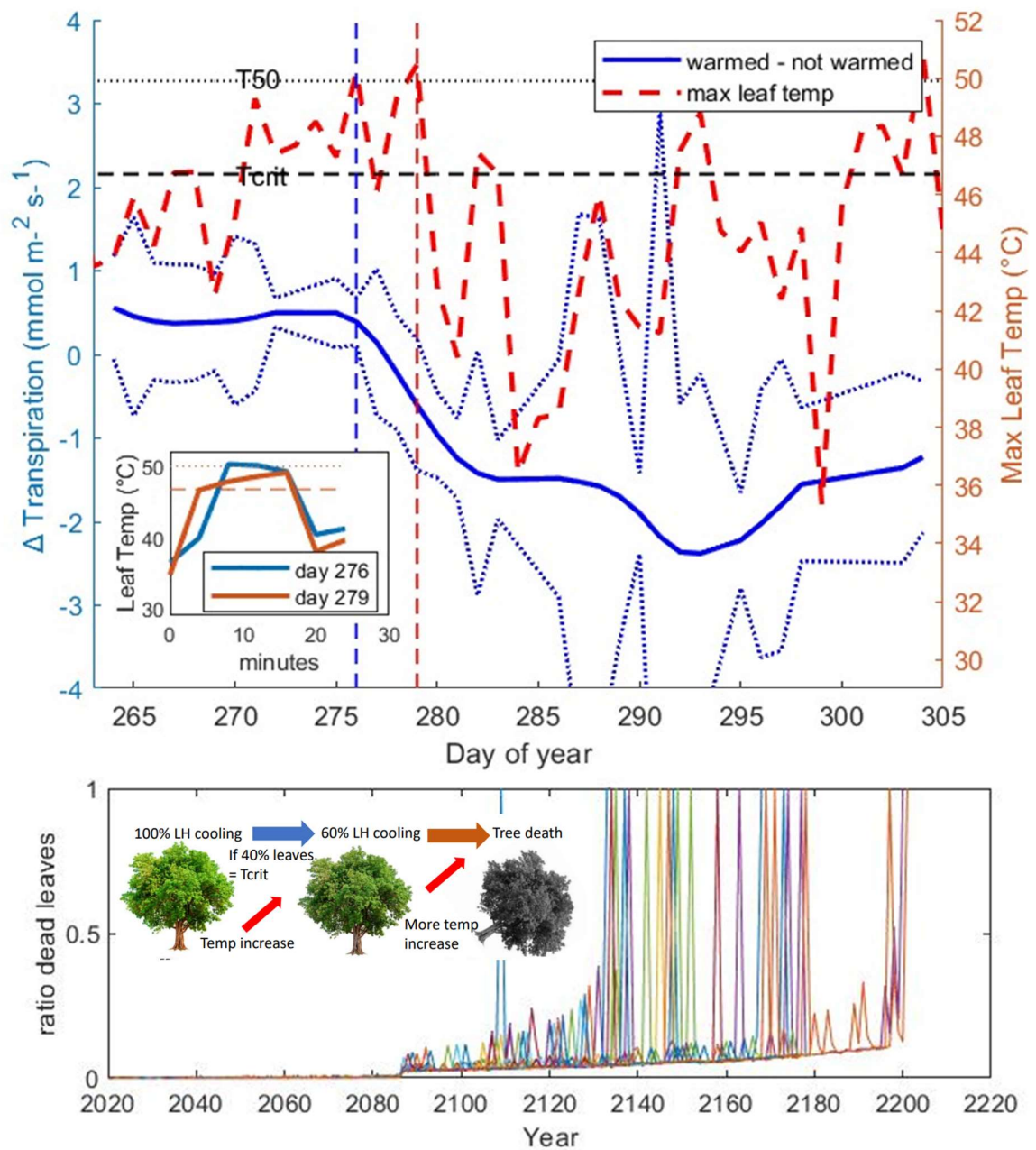
401

402 **Fig 1 – In situ and warming experiment leaf temperatures compared to canopy**
 403 **temperatures** - (A) Diurnal temperature patterns for the dry season (DS) for a region (SI Fig 1a)
 404 of the Amazon basin using ECOSTRESS data (green). Average canopy (solid line) and 40 m air
 405 air temperatures (circles) from the km 83 eddy covariance tower for the dry season (red) and the wet
 406 season (blue) for sunny periods (when $\text{solar}_{in}/\text{solar}_{in,max} > 90\%$ for the hour). (B) A histogram of
 407 individual canopy top leaf thermocouples from 11 individual leaves from the same site as “A”
 408 over 54 sunny periods lasting 20 minutes (measurements taken every 2 min) and the average of
 409 these data (33.2 °C). T_{crit} is the temperature when the photosynthetic machinery breaks down
 410 and is shown as a red line. (C) We aggregated all leaf thermocouple data from SI Figure 7 for
 411 ambient (blue) and warmed leaves (red) and show the percentage of leaves at +2 (Brazil), +3
 412 (Puerto Rico), and +4 °C (Australia) warming that were $>T_{crit}$. (D) Air temperature versus leaf
 413 temperature for a warming experiment for individual leaves (red dots), average leaf temperatures
 414 (blue circles), and one-to-one line (blue dotted).



415

416 **Figure 2 –Remotely sensed peak canopy temperature across the tropics** - Seasonal patterns
 417 of (A) soil moisture using SMAP and (B) canopy temperatures using ECOSTRESS for the
 418 Amazon basin (Fig ED1a red). For the hot dry period shown by the arrows, we show a larger
 419 spatial distribution (Fig ED1a green) (C) and log10 histogram focusing on the long tail of the
 420 data (D) using only the highest quality data flag. We show trends for periods of low soil
 421 moisture for (E) Southeast Asian region (Fig ED8) and (F) Central Africa (Fig ED7). G shows a
 422 world map with focal areas boxed in red.



423

424 **Figure 3 – Modelled impact of future warming on tropical forests -** (top) Warmed branch sap
 425 flow (N=9 branches) minus non-warmed (N=4 branches) sap flow (blue line) ± propagated error
 426 (blue dotted line) for sunny (irradiance >1200 mmol m⁻² s⁻¹) midday periods (10:30–14:00 h
 427 local time) on six tree species using passive black plastic heaters in a heating experiment
 428 conducted at Floresta Nacional do Tapajos, Brazil. Maximum daily temperatures for individual
 429 leaves (red stippled line) from a co-occurring leaf warming experiment during the same time
 430 period. Horizontal red lines indicate T_{crit} (dashed) and T₅₀ (dotted). The subset figure shows the
 431 duration of warm periods for day 276 and 279 (marked as vertical red and blue lines). Around

432 this period (between 276 and 279) transpiration decreases in warmed branches relative to the
 433 non-warmed branches. (bottom) Dead leaves as a ratio of total leaves over time with climate
 434 change for 30 simulations (one color per simulation). (Inset) Diagram of our model showing
 435 impact of T_{crit} on change in average canopy temperature as temperatures increase over time,
 436 where LH is latent heat. Tree image is from canva.com under a free content license.

437
 438
 439
 440
 441
 442

443 **Table 1– Current and future temperature extremes across the tropics.** The percent of time
 444 that canopy temperatures are estimated to exceed thresholds of ≥ 38.0 , 40.0 and 45.0 °C for low
 445 soil moisture regions of the Amazon, Central Africa, and Borneo. We then increase temperature
 446 by 2 °C to estimate the impact of climate change and show the same estimates for the three
 447 regions. Canopy temperatures are observed by ECOSTRESS and are limited to only the highest
 448 quality data.

449

	≥ 38.0 °C		≥ 40.0 °C		≥ 45.0 °C	
	Current	+2 °C	Current	+2 °C	Current	+2 °C
South America	0.50%	5%	0.10%	1%	0.00%	0.10%
Central Africa	0.60%	2%	0.06%	0.60%	0%	0.01%
SE Asia (Borneo)	3%	8%	1%	3%	0.01%	0.30%

450
 451
 452

453 **Table 2 –Results from model sensitivity studies.** An individual-based model showing
 454 estimated amount of climate change under different scenarios before leaf death. We first show
 455 results from the “most likely scenario” with an LAI of 5, 10% drought probability, 46.7 °C T_{crit},
 456 T_{crit} range=0, T_{crit} duration=1, a soil moisture exponent of -33.6, and maximum evaporative
 457 cooling of 4.4 °C. We then show the results of contrasting extreme scenarios as a means of a
 458 sensitivity analysis where we keep all other variables as in the “most likely scenario”, but vary
 459 the one mentioned. Temperature increase results represent means ± 1 SD, while time-scale
 460 results represent means and range in parentheses (n = 30 simulation runs).

Most likely scenario (T _{crit} =46.7)		Drought		T _{crit}		T _{crit} range	T _{crit} duration	Soil moisture coefficient	Max evap cooling
	LAI 5	20%	5%	45 °C	49.9 °C	46.7 ± 2 °C	>3 periods	-38.2	3.7 °C
Total temperature increase (°C)	3.9 ± 0.5	3.6 ± 0.7	4.9 ± 1.1	2.6 ± 0.6	7.3 ± 0.8	3.9 ± 0.7	4.7 ± 0.8	4.1 ± 0.7	5.2 ± 0.5
Time scale until leaf death (years)	132 (102- 163)	120 (88- 170)	163 (108 - 238)	89 (69- 133)	244 (204- 300)	131 (100 - 185)	159 (129- 220)	138 (91- 183)	173 (145- 202)

461
462

463

464 **Methods**

465 **Field Data** - We estimate canopy temperature at the km 83 eddy covariance tower in the Tapajos
466 region of Brazil¹⁻³ using a pyrgeometer (Kipp and Zonen, Delft, Netherlands) mounted at 64 m
467 to measure upwelling longwave radiation ($L \uparrow$ in $W m^{-2}$) with an estimated radiative-flux
468 footprint of $8,000 m^2$ ⁴. Data were collected every 2 seconds and averaged over 30-minute
469 intervals between August 2001 and March 2004. We estimated canopy temperature with the
470 following equation:

471 **Eq 1** – Canopy temperature ($^{\circ}C$) = $(L \uparrow / (E * 5.67e-8))^{0.25} - 273.15$

472 We chose an emissivity value (E) of 0.98 for the tower data, as this was the most common value
473 used in the ECOSTRESS data (SDS_Emis1-5 (ECO2LSTE.001) and the broader literature for
474 tropical forests⁵. We compared canopy temperature derived from the pyrgeometer to eddy
475 covariance derived latent heat fluxes (flux footprint $\sim 1 km^2$), air temperature at 40 m, which is
476 the approximate canopy height (model 076B, Met One, Oregon, USA; and model 107,
477 Campbell Scientific, Logan, Utah, USA) and soil moisture at depths of 40 cm (model
478 CS615, Campbell Scientific, Logan, Utah, USA). Further details on instrumentation and
479 eddy covariance processing can be found in^{1,3}. This site was selectively logged, which had a
480 minor overall impact on the forest⁶, but did not affect any trees near the tower.

481 *Leaf thermocouple data* - We measured canopy leaf temperature at a 30 m canopy walk-up tower
482 between July to December of 2004 and July to December of 2005 at the same site. We initially
483 placed 50 thermocouples on canopy-exposed leaves of *Sextonia rubra*, *Micropholis sp.*, *Lecythis*
484 *lurida*) (originally published in Doughty and Goulden 2008). Fine wire thermocouples (copper
485 constantan 0.005 Omega, Stamford, CT) were attached to the underside of leaves by threading
486 the wire through the leaf and inserting the end of the thermocouple into the abaxial surface. The
487 thermocouples were wired into a multiplexer attached to a data logger (models AM25T and 23X,
488 Campbell Scientific, Logan, UT, USA) and the data were recorded at 1 Hz. Additional upper-
489 canopy leaf thermocouple data from Brazil⁷, Puerto Rico⁸, Panama⁹, Atlantic forest Brazil¹⁰ and
490 Australia¹¹, were generally collected in a similar manner.

491
492 **Satellite data** - *ECOSTRESS data* (ECO2LSTE.001) – The ECOSystem Spaceborne Thermal
493 Radiometer Experiment on Space Station (ECOSTRESS) mission is a thermal infrared (TIR)
494 multispectral scanner with five spectral bands at 8.28, 8.63, 9.07, 10.6, and 12.05 μm . The
495 sensor has a native spatial resolution of 38 m x 68 m, resampled to 70 m x 70 m, and a swath
496 width of 402 km (53°). Data are collected from an average altitude of 400 ± 25 km on the
497 International Space Station (ISS). ECOSTRESS is an improvement over other thermal sensors
498 because no other sensors provide TIR data with sufficient spatial, temporal, and spectral
499 resolution to reliably estimate LST at the local-to-global scale for a diurnal cycle¹². To ensure
500 the highest quality data, we used ECOSTRESS quality flag 3520, which identifies the best
501 quality pixels (no cloud detected), a minimum-maximum difference (MMD) indicative of
502 vegetation or water¹³, and nominal atmospheric opacity. We accessed ECOSTRESS LST data
503 through the AppEEARS website (<https://lpdaac.usgs.gov/tools/appeears/>) for the following
504 products and periods: SDS_LST (ECO2LSTE.001) from a long longitudinal swath of the
505 Amazon for 25 December 2018 to 20 July 2020 (SI Fig 1a red box) and then a larger area of the

506 western Amazon for 18 September to 29 September 2019 (SI Fig 1a green box), Central Africa
507 for 1 August to 30 August 2019 (SI Fig 1b), and SE Asia for 15 January to 30 February 2020 (SI
508 Fig. 1c). The dates were chosen as all ECOSTRESS data available at the start of the study for
509 the smaller regions and for warm periods with low soil moisture for the larger areas. We
510 calculated “peak median,” which is defined as the average of the highest three medians of each
511 granule (i.e., for the Amazon SI Fig. 1a, there were 934 granules) for each hour period.

512 *Comparison of LST data* – We compared ECOSTRESS LST to VIIRS LST (VNP21A1D.001)
513 and MODIS LST (MYD11A1.006). A more detailed comparison and description of these sensors
514 can be found in Hulley et al 2021¹⁴. Details for the sensors and quality flags used are given in
515 Table S1. Broadly, G1 for ECOSTRESS and VIIRS is classified as vegetation (using emissivity)
516 and of medium quality. G2 is classified as vegetation, but of the highest quality. MODIS
517 landcover classifies this region as almost entirely broadleaf evergreen vegetation, but using
518 MMD (emissivity) only 18% (VIIRS) and 12% (ECOSTRESS) of the data are classified as
519 vegetation, rather than as soils and rocks (Table S2). Therefore, we use the vegetation
520 classification (from MMD) as a very conservative estimate of complete forest canopy cover and
521 not farms, urban, or degraded forest where rocks or soils are more likely to appear to satellites.

522 *SMAP data* – To estimate pantropical soil moisture, we use the Soil Moisture Active Passive
523 (SMAP) sensor and the product Geophysical_Data_sm_rootzone (SPL4SMGP.005). SMAP
524 measurements provide remote sensing of soil moisture in the top 5 cm of the soil¹⁵ and the L4
525 products combine SMAP observations and complementary information from a variety of
526 sources. We accessed SMAP data from the AppEEARS website for the following products and
527 periods: Amazon for 25 December 2018 to 20 July 2020 (SI Fig 1a), Central Africa for 25
528 December 2019 to 20 July 2020 (SI Fig 1b), and Borneo for 25 December 2018 to 20 July 2020
529 (SI Fig 1c).

530 **Warming experiments** – For model validation, we used the results of three upper-canopy leaf
531 and branch warming experiments of 2°C (Brazil)⁷, 3°C (Puerto Rico)⁸, and 4°C (Australia)¹¹.
532 The first experiment (Brazil), were 4 individual leaf resistant heaters on each of 6 different
533 upper-canopy species at the Floresta Nacional (FLONA) do Tapajos as part of the Large-Scale
534 Biosphere–Atmosphere Ecology Program (LBA-ECO) in Santarem, Brazil¹⁴. On the same six
535 species, black plastic passively heated branches by an average ~2°C. Initially, heat balance sap
536 flow sensors and the passive heaters were added to 40 branches, but we had confidence in the
537 data from 9 heated and 4 control in the final analysis. The second experiment (Puerto Rico) had
538 two species (*Ocotea sintenisii* (Mez) Alain and *Guarea guidonia* (L.) Sleumer where leaves were
539 heated by 3 °C at the Tropical Responses to Altered Climate Experiment (TRACE) canopy tower
540 site at Sabana Field Research Station, Luquillo, Puerto Rico⁸. The final experiment (Australia),
541 which increased leaf temperatures by 4 °C, was conducted at Daintree Rainforest Observatory
542 (DRO) in Cape Tribulation, Far North Queensland, Australia¹¹. Leaf heaters were installed using
543 a pair of 30-gauge copper-constantan thermocouples, one reference leaf and one heated with a
544 target temperature differential of 4 °C. There were two pairs in the upper canopy of each tree
545 crown installed in 2-3 individuals across four species with the thermocouples installed on the
546 underside of the leaves. Two absolute 36-gauge copper-constantan thermocouples were installed
547 in each species to measure the leaf temperatures of the reference leaves. Thermocouple wires

548 connected into an AM25T multiplexer from Campbell Scientific connected to a CR1000
549 Campbell datalogger. More details about the experiment and sensors can be found in ¹⁶.

550

551 **Model** – We created a model of individual leaves on a tree (100 by 100 grid where each leaf is a
552 pixel) using matlab (mathworks version 2022a) to estimate the upper limit of tropical canopy
553 temperatures with projected changes in climate. At the start of the simulation, we randomly
554 applied the measured distribution (ambient Fig 1c) of canopy leaf temperatures >31.2 °C (chosen
555 to give a mean canopy temperature of 33.2 ± 0.4 °C, matching the canopy average Fig 1b) to the
556 entire grid. Each year we increased the mean air temperatures by 0.03 °C to simulate a warming
557 planet. As air temperatures reached $+2$, 3 and 4 °C, we applied the leaf temperature distributions
558 (but subtracted out the air temperature increases) from the different warming experiments ($+2$ °C
559 (Brazil), $+3$ °C (Puerto Rico), and $+4$ °C (Australia), respectively (Fig ED4)). We ran the model
560 at a daily time step with leaves flushing once a year (all dead leaves reset to living each year).

561 In addition, to take into account the effect of climate inter-annual variation - specifically drought,
562 these mean canopy temperatures were further increased or decreased by deviations from mean
563 maximum air temperatures at 40 m pulled each day from the Tapajos eddy covariance tower¹⁻³
564 and soil moisture at 40 cm depth ($\text{m}^3 \text{m}^{-3}$) which controlled canopy temperatures following
565 equation 2 (Fig ED3a).

566 **Eq 2** – Canopy temperature (°C) = $46.5 - 33.6 * \text{soil moisture} (\text{m}^3 \text{m}^{-3})$

567

568 For example, in a non-drought year, on a day where max air temperatures were 0.1 °C higher
569 than average and soil moisture was $0.01 \text{ m}^3 \text{m}^{-3}$ lower than average (which would add 0.3 °C to
570 canopy temperatures (Eq 2)), we would add 0.4 °C to the grid canopy temperature that day.
571 Every year, there was a 10% random probability of either a minor (80% probability) drought
572 which reduced soil moisture by $0.1 \text{ m}^3 \text{m}^{-3}$ and increased air temperatures by 0.5 °C or severe
573 drought (20% probability), which reduced soil moisture by $0.2 \text{ m}^3 \text{m}^{-3}$ and increased air
574 temperatures by 1 °C. This is similar to the Amazon-wide temperature increases during the last
575 El Niño ¹⁷.

576 If an individual leaf temperature increases to above 46.7 °C (T_{crit}) the leaf died, following Slot et
577 al. (2021). Prior research has suggested that irreversible damage could begin at 45 °C ¹⁸ and T_{50}
578 for tropical species is 49.9 °C ¹⁹, and we use these values in a sensitivity study. We further
579 explore the impact of duration of T_{crit} on mortality in a sensitivity study (ranging between
580 needing a single exposure to four exposures to T_{crit} to die). Over the season, if a leaf died, then it
581 did not contribute towards canopy evapotranspiration. We ran simulations as a 3D canopy with
582 an LAI of 5 where if the top leaf died, then it was replaced by a shade-adapted leaf with a T_{crit} 1
583 °C lower ²⁰. If each of the 5 LAIs died, then all leaves in that grid cell were dead and canopy
584 evaporative cooling decreased by that percentage. Several lines of evidence suggest that under
585 normal hydraulic conditions, when radiation load increases from ~ 350 to 1100 W m^{-2} (e.g.
586 between shady and sunny conditions) average canopy temperature increases by ~ 3 °C and
587 therefore, evaporative cooling for a full 1100 W m^{-2} is ~ 4.4 °C^{4,21} (we vary this in a sensitivity
588 study between 3.7 and 5.1 °C). For example, if, over a year, 1000 leaves (10% of all leaves)
589 surpass T_{crit} and die, evaporative cooling for all leaves in the grid will be reduced by 10%
590 ($1000/(100 \text{ by } 100 \text{ grid})$) or 0.44 °C and 0.44 °C will be added to mean canopy temperature.

591 Therefore, mean canopy temperature could heat up by a maximum of 4.4°C either due to a
592 reduction of soil moisture or from an increase in dead leaves. We ran each simulation until the
593 point where all leaves were dead and repeated this 30 times. We assumed loss of tree function
594 following the death of all leaves, but we discuss this further in the discussion. We then ran
595 sensitivity studies for several of the key variables (bold indicates the standard model parameter)
596 including: drought (0.05, **0.1**, to 0.2 m³ m⁻³ decrease in soil moisture), change in T_{crit} (T_{crit}: 45,
597 **46.7**, 49.9 °C), T_{crit} range (100 by 100 grid =random distribution of 46.7±2, **100 by 100 grid**
598 **=46.7±0**), Max evaporative cooling (3.7, **4.4**°C), (T_{crit} duration (**exceed Tcrit once**, exceed
599 Tcrit more than 3 times) and soil moisture coefficient (**-33.6** -38.2; i.e. change the slope from Fig
600 ED2a by ± 1 sd).

601

602 Data availability – We provide key data as an attachment: Fig1leaftempshared.csv, Fig2data.csv,
603 Fig3data.csv

604 Code availability - Data and code to produce all figures are available at the following link-
605 URL: <https://doi.org/doi:10.5061/dryad.fqz612jx1>.

606

607

608 **Methods References**

- 609 41. Miller, S. D. *et al.* BIOMETRIC AND MICROMETEOROLOGICAL
610 MEASUREMENTS OF TROPICAL FOREST CARBON BALANCE. *Ecol. Appl.* **14**,
611 114–126 (2004).
- 612 42. da Rocha, H. R. *et al.* SEASONALITY OF WATER AND HEAT FLUXES OVER A
613 TROPICAL FOREST IN EASTERN AMAZONIA. *Ecol. Appl.* **14**, 22–32 (2004).
- 614 43. Goulden, M. L. *et al.* DIEL AND SEASONAL PATTERNS OF TROPICAL FOREST
615 CO₂ EXCHANGE. *Ecol. Appl.* **14**, 42–54 (2004).
- 616 44. Kivalov, S. N. & Fitzjarrald, D. R. Observing the Whole-Canopy Short-Term Dynamic
617 Response to Natural Step Changes in Incident Light: Characteristics of Tropical and
618 Temperate Forests. *Boundary-Layer Meteorol.* **173**, 1–52 (2019).
- 619 45. Jin, M. & Liang, S. An Improved Land Surface Emissivity Parameter for Land Surface
620 Models Using Global Remote Sensing Observations. *J. Clim.* **19**, (2006).
- 621 46. Miller, S. D. *et al.* Reduced impact logging minimally alters tropical rainforest carbon and
622 energy exchange. *Proc. Natl. Acad. Sci.* **108**, 19431 LP – 19435 (2011).
- 623 47. Doughty, C. E. An In Situ Leaf and Branch Warming Experiment in the Amazon.
624 *Biotropica* **43**, 658–665 (2011).
- 625 48. Carter, K. R., Wood, T. E., Reed, S. C., Butts, K. M. & Cavaleri, M. A. Experimental
626 warming across a tropical forest canopy height gradient reveals minimal photosynthetic
627 and respiratory acclimation. *Plant. Cell Environ.* **44**, 2879–2897 (2021).
- 628 49. Rey-Sanchez, A. C., Slot, M., Posada, J. & Kitajima, K. Spatial and seasonal variation of
629 leaf temperature within the canopy of a tropical forest. *Clim. Res.* **71**, 75–89 (2016).
- 630 50. Fauset, S. *et al.* Differences in leaf thermoregulation and water use strategies between
631 three co-occurring Atlantic forest tree species. *Plant. Cell Environ.* **41**, 1618–1631 (2018).
- 632 51. Crous, K. Y. *et al.* Similar patterns of leaf temperatures and thermal acclimation to
633 warming in temperate and tropical tree canopies. *Tree Physiol.* tpad054 (2023)
634 doi:10.1093/treephys/tpad054.
- 635 52. Xiao, J., Fisher, J. B., Hashimoto, H., Ichii, K. & Parazoo, N. C. Emerging satellite
636 observations for diurnal cycling of ecosystem processes. *Nat. Plants* **7**, 877–887 (2021).
- 637 53. Kealy, P. S. & Hook, S. J. Separating temperature and emissivity in thermal infrared
638 multispectral scanner data: implications for recovering land surface temperatures. *IEEE*
639 *Trans. Geosci. Remote Sens.* **31**, 1155–1164 (1993).
- 640 54. Hulley, G. C. *et al.* Validation and Quality Assessment of the ECOSTRESS Level-2 Land
641 Surface Temperature and Emissivity Product. *IEEE Trans. Geosci. Remote Sens.* **60**, 1–23
642 (2022).
- 643 55. Reichle, R., Lannoy, G. De, Koster, R. D., Crow, W. T. & 2017., J. S. K. SMAP L4 9 km
644 EASE-Grid Surface and Root Zone Soil Moisture Geophysical Data, Version 3. Boulder,
645 Color. USA. NASA Natl. Snow Ice Data Cent. Distrib. Act. Arch. Center. doi
646 <https://doi.org/10.5067/B59DT1D5UMB4>. (2017).
- 647 56. Crous KY *et al.* Similar patterns of leaf temperatures and thermal acclimation to warming
648 in temperate and tropical tree canopies. In review.
- 649 57. Jiménez-Muñoz, J. C. *et al.* Record-breaking warming and extreme drought in the
650 Amazon rainforest during the course of El Niño 2015–2016. *Sci. Rep.* **6**, 33130 (2016).
- 651 58. Berry, J. & Bjorkman, O. Photosynthetic Response and Adaptation to Temperature in
652 Higher Plants. *Annu. Rev. Plant Physiol.* **31**, 491–543 (1980).
- 653 59. Slot, M. *et al.* Leaf heat tolerance of 147 tropical forest species varies with elevation and

- 654 leaf functional traits, but not with phylogeny. *Plant. Cell Environ.* **44**, (2021).
655 60. Slot, M., Krause, G. H., Krause, B., Hernández, G. G. & Winter, K. Photosynthetic heat
656 tolerance of shade and sun leaves of three tropical tree species. *Photosynth. Res.* **141**, 119–
657 130 (2019).
658 61. Doughty, C. E. & Goulden, M. L. Are tropical forests near a high temperature threshold?
659 *J. Geophys. Res. Biogeosciences* (2009) doi:10.1029/2007JG000632.
660
661

662 **Acknowledgements** - Support was provided by the ECOSTRESS mission and NASA Research
663 Opportunities in Space and Earth Science grants # 80NSSC20K0216, 80NSSC19K0206 and
664 80NSSC21K0191. SF and EG acknowledge Natural Environmental Research Council
665 NE/V008366/1. KC acknowledges the Australian Research Council DE160101484.
666

667 **Author contributions** – CED, GG, IO, YM, and JF designed the study. CED and JK analyzed
668 the RS data. CED, MG, HR, SM, SF, EG, CRS, MS, KRC, KYC, KM and AWC collected and
669 analyzed the empirical data. CED created the model. CED and BCW prepared the public data
670 and code. CED wrote the paper with contributions from GG, KRC, JF, and IO.

671 **Additional Information:** Supplementary Information is available for this paper.

672 Correspondence and requests for materials should be addressed to chris.doughty@nau.edu.

673 Reprints and permissions information is available at www.nature.com/reprints

674 The authors declare no competing interests.

675

676

677 **Extended data figure captions**

678 **Fig ED 1 – Regions of interest.** Tropical forest regions in A) Amazon, B) Central Africa and C)
679 SE Asia used for the retrieval of ECOSTRESS LST and SMAP data. The red area was used to
680 ground-truth ECOSTRESS LST with the pyrgeometer.

681
682 **Fig ED 2 – Impacts on canopy temperature.** (A) Linear regression of canopy temperature
683 versus soil moisture (40 cm depth) at the km 83 eddy covariance tower ($r^2 = 0.46$, $P=7e-10$,
684 $N=62$). (B) Linear regression of canopy temperature as a function of air temperature during
685 sunny periods during the wet (green circles) and dry (red circles) season at the km 83 eddy
686 covariance tower in the Tapajos region of Brazil. Red line shows a linear fit for the dry season
687 ($r^2 = 0.96$, $P=3e-21$, $N=29$) and the lower line is a one-to-one line. (C) Linear regressions of
688 canopy temperature as a function of latent heat flux for warm ($>30^\circ\text{C}$) periods ($r^2=0.50$, $P=0.009$,
689 $N=11$) at the km 83 eddy covariance tower in the Tapajos region of Brazil. (D) Linear regression
690 ($r^2=0.75$, $P=2e-5$, $N=16$) using data from Figure 1a comparing ECOSTRESS dry season to
691 pyrgeometer dry season data from the Tapajos (Km 83).

692
693 **Fig ED 3 – Histograms of canopy temperature.** Histograms of the canopy temperatures as
694 (top) 30 min average periods and (bottom) two second instantaneous observations, where total
695 shortwave energy load is $>1000 \text{ W m}^{-2}$, as measured by a downward facing pyrgeometer in the
696 Tapajos region of Brazil.

697
698 **Fig ED 4 – Leaf thermocouple data from warming experiments.** Canopy top tropical leaf
699 thermocouple measurements for normal (blue) and warmed leaves (red) for Brazil ($+2^\circ\text{C}$) (a),
700 Puerto Rico ($+3^\circ\text{C}$) (b), and Australia ($+4^\circ\text{C}$) (c). Insets show the long tail distribution of
701 temperatures and text records the highest leaf temperature.

702
703 **Fig ED 5 – Leaf thermocouple data.** Canopy top tropical leaf thermocouple measurements for
704 (top) Brazil km 67, (middle) Panama and (bottom) the Atlantic Forest in Brazil. Insets show the
705 long tail distribution of temperatures and text records the highest leaf temperature. The
706 resampled assumes a similar number of samples ($\sim N=400$) at 38°C for both sites and fits a curve
707 to extrapolate the long tail. The Atlantic forest is a cooler forest (at $\sim 1000\text{m}$) and the median
708 temperature of the Amazon is $\sim 4^\circ\text{C}$ higher than the Atlantic forest.

709
710 **Fig ED 6 –Duration of warming.** Periods when the leaves were warmed by >8 minutes during
711 the Tapajos warming experiment for individual leaves (thin lines) and averaged (thick red line).
712 Text in figure indicates the percent of time leaves exceeded T_{crit} for greater than 6 and 8
713 minutes.

714
715 **Fig ED 7–Finding African peak temperatures.** Procedure for finding peak canopy
716 temperatures using ECOSTRESS data for central Africa. (A) Histogram of temperatures for (B)
717 a region of Central Africa. A diurnal curve showing all ECOSTRESS LST data for central
718 Africa versus (C) time of day and (D) time of year. (E) SMAP soil moisture ($\text{m}^2 \text{ m}^{-2}$) data
719 showing periods of (red lines) dry weather.

720
721 **Fig ED 8 - Finding SE Asian peak temperatures.** Procedure for finding peak canopy
722 temperatures using ECOSTRESS data for SE Asia. (A) Histogram of temperatures for (B) a

723 region of SE Asia. A diurnal curve showing all ECOSTRESS LST data for SE Asia versus (C)
724 time of day and (D) time of year. (E) SMAP soil moisture data ($m^2 m^{-2}$) showing periods of (red
725 lines) dry weather.

726

727 **Fig ED 9 – Comparison of LST temperature data.** We show the spatial distribution of LST
728 data for three sensors (VIIRS, MODIS, and ECOSTRESS) for similar time periods (Sept 18-28,
729 2019) for similar areas in the Amazon basin. The difference between the left, middle and right
730 are different data quality flags for no flag (left), QF g1 from Table S1 (middle) and QF g2
731 (right). We used three levels of quality flags (ECOSTRESS – G1 - 3522 and 3520, G2 =3520,
732 VIIRS – G1 – 12001, 15841, 11745, 32225 and G2 = 32225, and MODIS – G1 - 0 and 65 and
733 G2 -0) for the region depicted in SI Fig 1b during the same period (18 September to 28
734 September 2019). Quality flags were complex with 136 for ECOSTRESS and 229 for VIIRS
735 (but only 8 for MODIS).

736

737 **Fig ED 10 – Histogram of LST temperature data.** (top) We show histograms of LST data for
738 three sensors (VIIRS, MODIS, and ECOSTRESS) for similar time periods (Sept 18-28, 2019)
739 for similar areas in the Amazon basin. The difference between the left, middle and right are
740 different data quality flags for no flag (left), QF g1 from Table S1 (middle) and QF g2 (right).
741 We used three levels of quality flags (ECOSTRESS – G1 - 3522 and 3520, G2 =3520, VIIRS –
742 G1 – 12001, 15841, 11745, 32225 and G2 = 32225, and MODIS – G1 - 0 and 65 and G2 -0) for
743 the region depicted in SI Fig 1b during the same period (18 September to 28 September 2019).
744 (bottom) - A scaled in comparison for the same dataset showing the much higher resolution of
745 ECOSTRESS versus VIIRS and MODIS LST.

746

747